Mathematical Modeling of T-Cell Receptor Triggering and Activation

Sumeet Agarwal*
Supervisors: Kevin Burrage*, Simon Davis*

June 24, 2008

Abstract

T-cells form a crucial component of the immune system, and play a key role in the development of adaptive immunity. On stimulation by foreign peptides, they differentiate into specialized helper and cytotoxic T-cells which orchestrate the adaptive immune response. In this project, we looked at the molecular basis of T-cell activation; in particular, mathematical modeling of the reaction kinetics between receptors on the T-cell surface and their ligands on an antigen-presenting cell. The first part of the project consisted of examining existing models for T-cell activation and costimulation (signaling via receptors other than the main T-cell receptor), and attempting to integrate these. In the second part, we wrote down a novel set of equations to describe part of the chemical kinetics at the initiation of contact between a T-cell and an antigen-presenting cell, based on existing stoichiometric, binding affinity and expression data. We used our model to carry out both deterministic and stochastic simulations of these kinetics. Our results indicate that amongst the qualitative models proposed in the literature for T-cell receptor (TCR) triggering, a model of "pseudodimerization" of TCRs is unlikely to be accurate, whereas "kinetic segregation" based triggering of single TCRs is better supported by existing data.

1 Introduction

In order to effectively fight the wide range of pathogens that any given individual will encounter over the course of a lifetime, the lymphocytes of the adaptive immune system (of which there are two types, B-cells and T-cells) have evolved to be able to recognise a huge variety of different antigens from bacteria, viruses and other disease-causing organisms (Murphy et al., 2008). Whilst B cells secrete immunoglobulin molecules known as antibodies which bind to specific pathogens or their toxic products, T cells are the key controllers of cell-mediated immunity, and are marked out by the presence of a special membrane-bound receptor known as the T-cell receptor (TCR). The TCRs are structurally and functionally similar to immunoglobulins; however, they do not bind directly to antigens, but instead recognize short peptide fragments of specific protein antigens, which are bound to proteins called MHC molecules (since they are encoded in a cluster of genes known as the Major Histocompatibility Complex) on the surfaces of infected cells. These cells are referred to as Antigen Presenting Cells (APCs). There are two classes of MHC molecules, I and II, which are recognised respectively by two distinct T-cell co-receptors, known as CD8 and CD4.

Once the TCR has recognised and bound to the peptide-MHC (pMHC) complex on an APC, it leads to activation of the T-cell, with a sequence of downstream events leading to the immune response. However, full-fledged activation of a T-cell requires not only TCR binding to a specific antigen peptide, but also the non-specific binding of two other T-cell membrane receptors, CD28 and CTLA-4, to their shared ligands on APCs, B7-1 and B7-2. This latter process is known as costimulation, and a mathematical model attempting to elucidate its chemical kinetics has recently been proposed (Jansson et al., 2005). In the first part of the project, we looked at this model and implemented it in order to reproduce the results. We also attempted to integrate the model into a broader one that has very recently been published, and attempts to account for the entire sequence of steps leading from TCR-pMHC binding to T-cell activation and response (Bidot et al., 2008). The latter model is seemingly

*sumeet.agarwal@dtc.ox.ac.uk, kevin.burrage@comlab.ox.ac.uk, simon.davis@ndm.ox.ac.uk

lacking in several of the key details of costimulation, so adding the former into it appeared to be appropriate. These two models, along with details of how we combined them and the results thereof, are dealt with in Section 2.

Having examined the broad-ranging model of T-cell activation mentioned above (Bidot et al., 2008), we felt that it was lacking in too many important details and oversimplifying the system too much to be of any real use. Given the evident complexity of the signaling pathways involved (see Section 2.2) and our very limited understanding of how they work, it seemed to be a better idea to focus on a narrower portion of the process in an attempt to explain it better. So in the second part of the project, we looked at the problem of 'TCR triggering', i.e., how engagement of the antigen by the TCR actually leads to initiation of the intracellular signaling that activates the T-cell. This is at present an unsolved problem, although several seemingly plausible mechanisms have been proposed. Two of the most prominent are known as 'pseudodimerization' (Irvine et al., 2002) and 'kinetic segregation' (Davis and van der Merwe, 1996). In order to examine the relative merits of these models given experimental data about stoichiometry and binding affinities, we developed a simple mathematical model of the chemical kinetics at the interface of a naïve (unactivated) T-cell and an APC, involving the TCRs, MHC molecules and another important T-cell membrane protein called CD4. One of the two 'co-receptors' CD4/CD8 is expressed by any given mature T-cell, determining its type: CD4 is carried by 'helper' cells, whose function is to activate other cells, while CD8 is carried by 'cytotoxic' cells, which directly kill infected cells. Here we have focused on helper T-cells. It has been shown for these that in the absence of CD4, sensitivity to antigenic peptide is substantially weakened (Irvine et al., 2002).

Using our model, we carried out both deterministic and stochastic simulations in Matlab, and looked at how well the results fit in with the two triggering mechanisms mentioned. Details of both hypotheses, our model and simulation results, along with a discussion of their implications, are in Section 3. Section 4 sums up the outcomes of this project and concludes the report.

2 Models for T-cell activation and downstream signaling

2.1 Costimulation

APCs that can activate naïve T cells bear membrane proteins known as co-stimulatory molecules, which interact with co-stimulatory receptors on the T cell surface in order to transmit the secondary signal which is required for activation, in addition to antigen binding to the TCR. The best-known co-stimulatory receptors are CD28 and CTLA-4, which both bind to ligands on APCs called B7-1 and B7-2. The precise role of these two receptors is not well understood. We looked at a mathematical model for simulating the accumulation of the four co-stimulatory molecules within the contact region between the membranes of a T cell and an APC, known as the immunological synapse. The model is based on a system of mean-field ordinary differential equations, parametrized by biophysical and expression data on the molecules involved. It is a compartment model, which breaks up the simulation region (i.e., the cell surface) into two parts, the synapse and the membrane region outside the synapse, allowing for diffusion between them. For details of the equations involved, see Jansson et al. (2005).

We implemented the 'free diffusion' version of the model, which allows a fraction of the molecules to diffuse freely at the cell surface. The Matlab code is given in Appendix A.1. Figure 1 shows the results of our simulations. From the graph of Figure 1(a), which essentially reproduces the results obtained by Jansson et al. (2005), one can see that B7-1 and B7-2 appear to be the dominant ligands for the CTLA-4 and CD28 receptors respectively. The key insight from this paper was that stoichiometry and competition effects can greatly influence complex formation at cellular interfaces. For instance, the results of Figure 1(a) were obtained by allowing multivalent interactions between CTLA-4 and B7-1, since both of these molecules are bivalent and thus it is expected that they can form long multivalent chains (see Figure 2 for an illustration). However, if we restrict interactions between CTLA-4 and B7-1 to being just bivalent (i.e., we allow B_1 and C_1 from Figure 2, but not E_2 or anything bigger), then we get a very different outcome, shown in Figure 1(b). Now, we find that B7-2 is the dominant ligand for CTLA-4, rather than B7-1. So the specificity of ligand-receptor interaction can be critically dependent on factors such as valency.

Next, we look at a framework which attempts to give a more comprehensive model of the T-cell activation process, and see how we can relate this costimulation model to that.

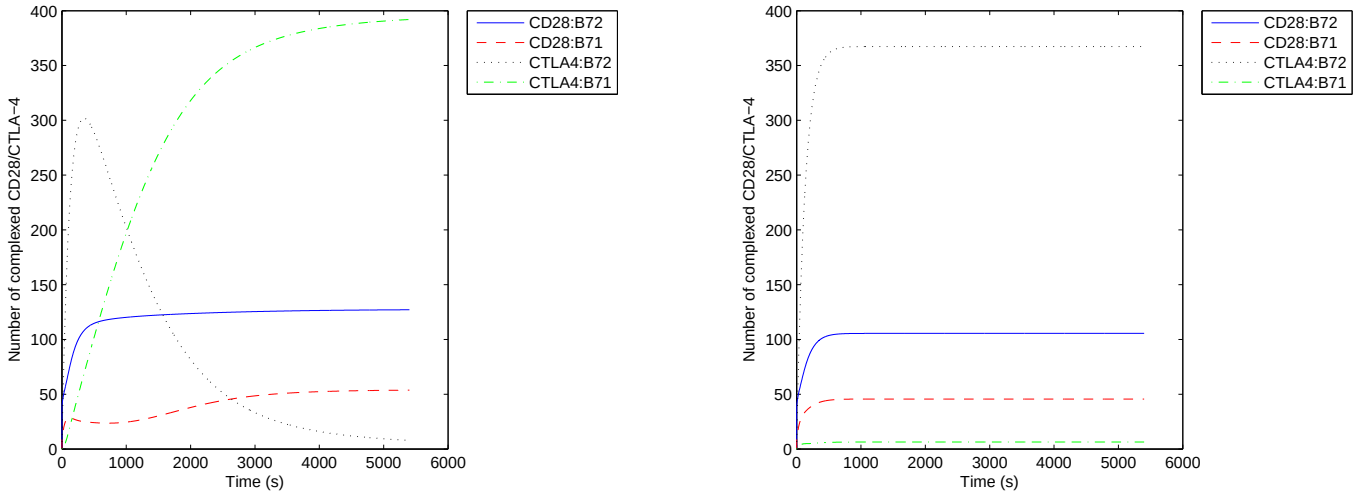

(a) CTLA-4:B7-1 Multivalent interaction

(b) CTLA-4:B7-1 Bivalent interaction

Figure 1: Complex formation in the costimulation model, with expected multivalent chain formation between CTLA-4 and B7-1 (left); allowing for only bivalent complex formation between them (right).

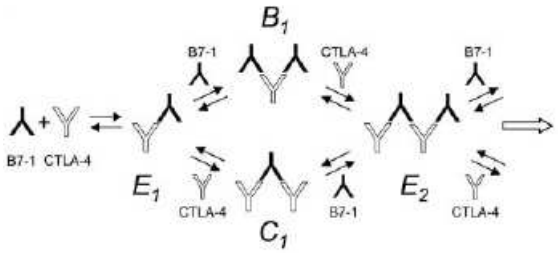

Figure 2: The bivalent nature of both B7-1 and CTLA-4 allows multivalent chains to build up when they are complexed.

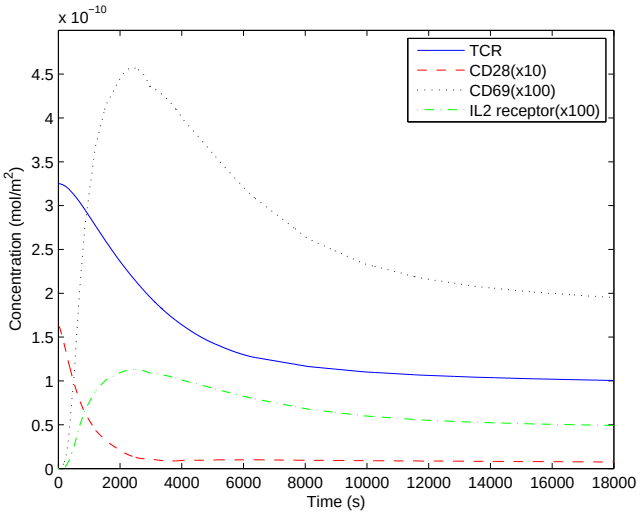

(a) Receptor levels inside the synapse

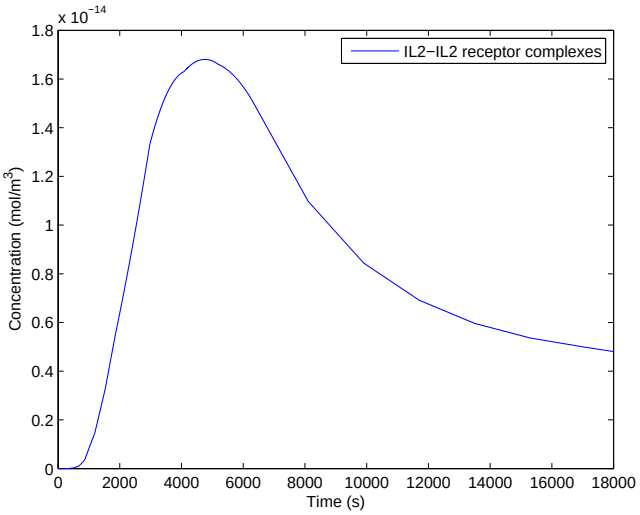

(b) IL2-IL2 receptor internalized activated complexes

Figure 3: Results of simulation using our implementation of the model of Bidot et al. (2008).

2.2 Activation leading to immune response

In a recent paper, Bidot et al. (2008) propose a mathematical model for the kinetics of T-cell activation. They look at a broad range of steps, starting from TCR-pMHC binding, followed by CD4/CD8 co-receptor binding leading to activation, which results in the production of new receptors known as CD69 and the Interleukin-2 (IL2) receptor, as well as secretion of IL2 itself. IL2 is a signaling molecule used to coordinate the response to infection by T cells. The model includes an amplification effect caused by costimulation, but considers only one costimulatory receptor, CD28.

We attempted to implement this model and reproduce the results reported in the paper. However, it was impossible to do so as the values of a large number of parameters had not been specified by the authors. Based on some estimated and guessed parameter values, we were able to obtain results qualitatively similar to those published. The Matlab code used for this is given in Appendix A.2. The results of our simulations are depicted in Figure 3.

Due to the oversimplified representation of the signal transduction process in the model, the simulation results do not seem to provide a great deal of new insight. At best, we get a rough overview of what happens during T-cell activation. The evolution of receptor levels inside the immunological synapse with time is shown in Figure 3(a). Only TCRs and CD28 are present initially on the naïve T cell, whilst CD69 and the IL2 receptor are generated after TCR activation. The levels of the former two receptors drop rapidly in the first hour or so as they engage their respective ligands, forming complexes which are then internalized. On the other hand, CD69 and the IL2 receptor rise rapidly as their production is triggered by TCR activation, then drop back as they themselves begin to form complexes which are internalized and degraded. After the first couple of hours, levels are seen to have nearly stabilized. Figure 3(b) depicts the concentration inside the T cell of activated and internalized complexes formed between IL2 and its receptor. As per the authors, this quantity is a measure of overall T cell activation. The graph shows that there is a biphasic response, with a very sharp initial increase followed by a drop and stabilization at a lower level.

Since this model did not include the costimulatory molecule CTLA-4, which is known to have an inhibitory effect as opposed to the amplification caused by CD28, we attempted to modify it by incorporating the more detailed model of costimulation discussed in the previous section. The results are covered below.

2.3 Integration of costimulation kinetics into activation model

The model of Jansson et al. (2005) simulates the kinetics of the costimulatory molecules, CD28 and CTLA-4, and how they are engaged in complexes by their shared ligands, B7-1 and B7-2. The activation model of Bidot et al. (2008) also includes costimulation, but in a much simpler way, with only CD28 and one ligand (B7-1), and assuming only monovalent interactions, whereas B7-1 is in fact believed to be bivalent. So we replaced the costimulation equations in the latter model (specifically, Equations (7)-(9) of Bidot et al. (2008)) with the free-diffusion version of the former. Parameters relating to cell geometry were set according to the costimulation model: T-cell radius at 6 μm, APC radius at 10 μm and synapse radius at 2 μm. Also, in order to model downstream effects of CTLA-4, which was the effective new component introduced to the T-cell activation framework, and is known to be an inhibitor rather than an activator, we added the following chemical equations to the overall model:

$$CTLA4 - C \xrightarrow{k_{f2}} CTLA4^{*}(+B71/B72) \tag{1}$$

$$CTLA4^{*} \xrightarrow{k_{i2}} CTLA4^{*i} \tag{2}$$

$$CTLA4^{*i} \xrightarrow{k_{d2}} \tag{3}$$

$$T^{*i} + CTLA4^{*i} \xrightarrow{k_{p1}+k_{p2}} \tag{4}$$

Here the term $CTLA4 - C$ represents the total amount of complexed CTLA-4: i.e., in monovalent and bivalent complexes with B7-2, and in complexes of all sizes with B7-1 (see Figure 2). As with other receptors in the activation model, we assume that engaged CTLA-4 is activated (1), internalized (2) and degraded (3), in that sequence. Also, in order to represent the inhibitory effect of the receptor, we assume that activated internalized CTLA-4 reduces the concentration of effective TCRs (4). All rate constants are taken to be the same as the corresponding ones for CD28 in the original model; in Equation (4), we sum up the rate constants for the two TCR-CD28 reactions (Equations (K13)-(K14) of Bidot et al. (2008)) under the assumption that activated CTLA-4 and CD28 engage equally with activated TCRs. The only other modification was that occurrences of $CD28 - B71$ complexes in the original activation model were replaced with total complexed CD28, as it too may engage with both B7-1 and B7-2.

The results of simulations carried out using this new model (Matlab code given in Appendix A.3) are shown in Figure 4. The first thing to note is that the graphs are quite similar to the ones for the original model; except for CD28, all other components display similar trends as before. CD28 is now seen to rise initially instead of falling, and stabilises at a much higher concentration. This is presumably due to different expression level and binding affinity values, which are now taken from the costimulation model. Also, competition for the same ligands with CTLA-4 may be influencing the CD28 dynamics. Figure 4(a) also shows that CTLA-4 follows a qualitatively similar trend to CD28; and the other key notable difference, compared to Figure 3(a), is that whilst the IL2 receptor curve has a similar shape, the actual concentration of the receptor is now nearly an order of magnitude lower. This is also reflected in Figure 4(b), which again displays a nearly 10-fold drop in concentration of internalized activated IL2 receptor complexes compared to Figure 3(b). Thus, it would appear that the introduction into the model of CTLA-4 has led to significant reduction in the T-cell activation levels, as measured by internalization levels of engaged IL2 receptors.

2.4 Discussion

In this part of the project we essentially implemented two existing models and then attempted to integrate them into one. The first model gave us a picture of the molecular processes that underlie costimulation, and demonstrated how a combination of factors, such as stoichiometry, affinities and competition for shared ligands, may result in ligand-receptor binding specificity. The results obtained support the hypothesis that B7-2 and B7-1 are the dominant ligands of CD28 and CTLA-4 respectively. The second model gave a mathematical framework for incorporating a number of different steps involved in the T-cell activation process, including costimulation. The simulation outcome for this model showed the trends that concentrations of different receptors may be expected to follow as a naïve T cell is being activated. However, these seemingly contribute little to our understanding of the mechanisms underlying the process; for instance, the model did not attempt to include any details of the signal transduction steps whereby triggered TCRs actually upregulate the production of molecules like CD69 and IL2.

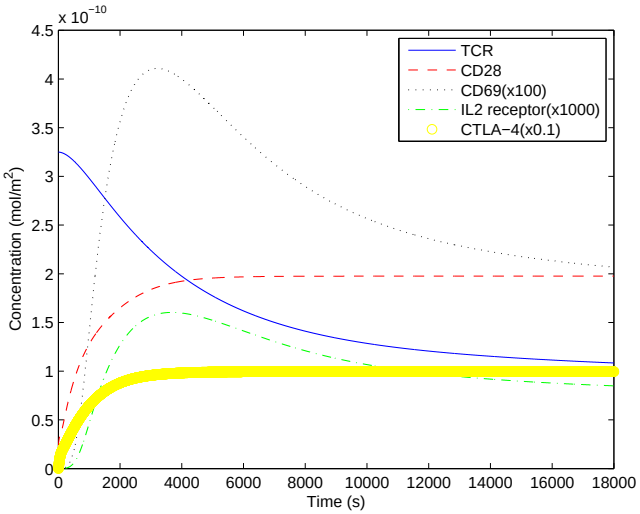

(a) Receptor levels inside the synapse

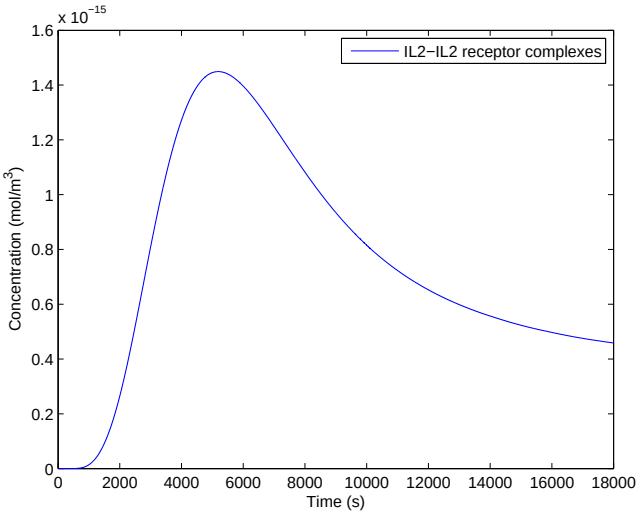

(b) IL2-IL2 receptor internalized activated complexes

Figure 4: Results of simulation using the modified costimulation-activation model.

The latter model also appeared to be missing several significant details: for instance, it did not include CTLA-4 and its inhibitory effect, nor did it allow for multivalent interactions during costimulation. As discussed in the previous section, we inserted the first model into the second in order to see what impact the additional detail would have. The results showed that introduction of TCR inhibition via CTLA-4 caused a large drop in the concentration levels of IL2 receptors, and thus presumably in the T cell activation levels. Once again, though, there is no elucidation of the mechanism by which the costimulatory receptors amplify or inhibit the immune response. As can be seen from Equation 4 above, the underlying biochemistry is encapsulated in just a single step; this sort of simplification appears throughout the activation model (Bidot et al., 2008). So at best we can say that the costimulatory kinetics of Jansson et al. (2005) are compatible with CTLA-4 having a major inhibitory role. The results obtained by us may not even be very meaningful, as the two models had somewhat differing assumptions about the cell's geometry and the diffusion mobility between the synapse and the outside, and whilst we have taken relevant parameter values preferentially from the costimulation model, some of these may be inappropriate under the assumptions of the other model.

On the whole, we felt that from the point of view of obtaining a more precise understanding of what is involved in T cell activation, it would be more productive to focus our attention on a smaller part of the process and attempt to model it in more detail. Thus, in the second part of the project we looked at just the first chapter of the story: how the T cell receptor is triggered.

3 T-Cell Receptor triggering

The initial step in the mounting of immune response via T cells is the engagement of antigenic peptide by the T-cell receptor. How this engagement occurs is known, but not how that 'triggers' intracellular signaling (Davis and van der Merwe, 2006). The TCR is a heterodimer and consists of two transmembrane glycoprotein chains, known as α and β. The ligand recognised by it is actually a complex of a specific peptide and an MHC molecule, where the peptide is a short fragment of a foreign protein; these proteins are unfolded and processed into fragments by antigen-presenting cells. The peptide-MHC complex is then presented on the APC surface, and the recognising TCR makes contacts with both the MHC molecule and the antigen

peptide (Murphy et al., 2008).

Once this recognition has happened, it somehow leads to the generation of signals that culminate in T-cell activation; this is what is known as TCR triggering. There are multiple theories of the mechanism behind this process (Krogsgaard and Davis, 2005). We will focus here on two of the more prominent ones, first describing their implications and then looking at a mathematical model which may help to favour one over the other.

3.1 Kinetic Segregation

The key idea behind kinetic segregation (Davis and van der Merwe, 1996) is that triggering happens due to spatial reorganization of signaling proteins. Figure 5 illustrates how this works. The TCR generally exists in complex with chains of a molecule known as CD3, and when these chains are phosphorylated they recruit a molecule called ZAP-70, which leads to further heavy phosphorylation and activation. In a resting T-cell, there is a balance between phosphorylation by kinases (like leukocyte-specific protein tyrosine kinase, or Lck) and dephosphorylation by phosphatases (like CD45), and thus no triggering occurs. When the T cell comes into contact with an APC, however, close-contact zones get created (similar to the immunological synapse discussed earlier, but believed to be much smaller), nucleated by the binding of the small CD2 co-receptor to its ligand CD58. Phosphatases like CD45 get excluded from these zones due to their large extracellular domains, and thus they become kinase-rich. If a TCR in one of these zones binds to its pMHC ligand, it is likely to be trapped there, allowing the phosphorylation of sites on the associated CD3 chains (known as immunoreceptor tyrosine-based activation motifs, or ITAMs). This then leads to triggering via ZAP-70 recruitment, as mentioned earlier. Thus, the exclusion of the phosphatases from the close-contact zones is what allows sufficient phosphorylation levels to be achieved for activation.

The distinguishing feature of this model is that it does not require a conformational change or dimerization of the TCR in order to account for triggering. There is no evidence for the former occurring, and the latter idea is problematic because it has been experimentally shown that just a single agonist (antigenic) peptide-MHC complex on an APC is able to trigger T-cell activation (Irvine et al., 2002). However, an alternative model known as 'pseudodimerization' was proposed to try and get around this issue; we discuss this next.

3.2 Pseudodimerization

The idea behind this model is that two bound TCRs can be brought together by the dual binding of a CD4 molecule. CD4 has an important role during activation, because it has been shown that whilst T cells containing CD4 are able to detect APCs with just a single ligand, T cells in which CD4 has been blocked via antibodies require at least 30 or so ligands to be present before they respond (Irvine et al., 2002). According to this model, the function of CD4 is to allow 'pseudodimers' to form between a TCR bound to an agonist and another one bound to a self-peptide. Typically, any given APC will be expressing around 50,000 MHC molecules, most of which are complexed with peptide fragments from endogenous proteins. Only a small fraction will have picked up foreign peptides. Of course, TCR binding to self-peptides is relatively very weak, which is what prevents autoimmune response. However, this model says that this weak interaction can be stabilized by the co-binding of a CD4 molecule. The process is depicted in Figure 6. It is assumed that many TCRs are closely associated with CD4s to begin with. When such a TCR binds an agonist, its attached CD4 can bind to a self-peptide which is also bound to another TCR, thus leading to the two TCRs being brought together into a pseudodimer. Whilst the interactions of the self-peptide with both the TCR and the CD4 are expected to be quite weak, the model assumes that the combination of these two weak interactions can lead to stability. Once a pseudodimer has formed, it is assumed to provide the initial triggering (since several other cell-surface receptors are known to cause activation by dimerization or aggregation), although the mechanism of this has not been elucidated. When CD4 is absent, the model says that actual dimerization of two agonist-bound TCRs must occur, and therefore the observation that larger quantities of ligand are required in this case.

Thus, whilst the kinetic segregation model allows for triggering based on single TCRs being engaged and held in the close-contact zone, the pseudodimerization model requires two TCRs to come together in the fashion described before activation can begin. We wrote down a set of chemical equations to try and mathematically model the processes of TCR, pMHC and CD4 binding, and based on known experimental data of expression levels and affinities, simulate what would actually happen when a T-cell and an APC came together. Our model is described below.

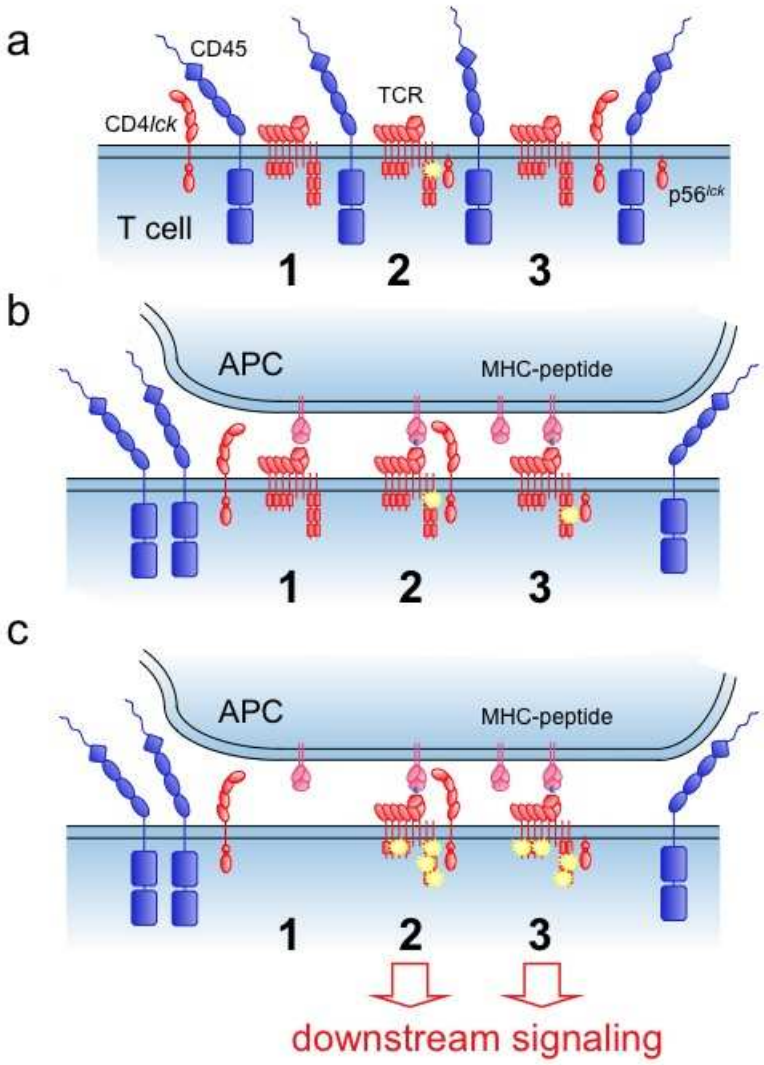

Figure 5: The kinetic-segregation model (Davis and van der Merwe, 1996). In a resting T-cell (a), there is a dynamic balance between phosphorylation by kinases (smaller molecules, such as lck) and dephosphorylation by phosphatases (bigger, like CD45). When the cell comes into contact with an APC (b), the binding of the small CD2 co-receptor to its ligand CD58 leads to a close-contact zone being created, from which the bigger phosphatases get excluded. Thus, a kinase-rich domain is created, where any engaged TCRs get trapped and phosphorylated (c).

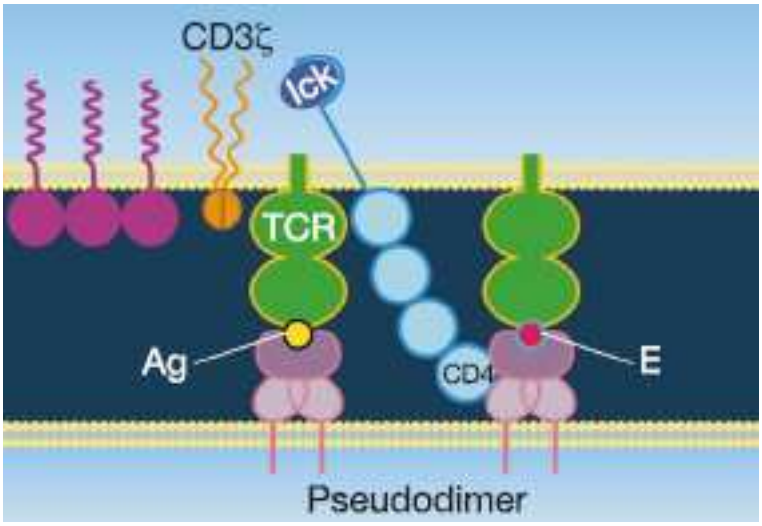

Figure 6: The pseudodimerization model (Irvine et al., 2002). A CD4 molecule is posited to act as a bridge between two engaged TCRs, one of which may only be weakly bound to a self-peptide (denoted by E; Ag denotes an agonist or foreign peptide).

3.3 Mathematical modeling of TCR binding kinetics

We chose to include just 4 basic components in our model, as we felt these were the ones relevant to evaluating the relative merits of the two triggering models discussed. The 4 components were:

- MHC molecules complexed with an agonist peptide on the APC (denoted by A)
- MHC molecules complexed with a self peptide on the APC (denoted by S)
- TCRs associated with a CD4 molecule on the T cell (denoted by TC)
- Unassociated TCRs (denoted by T)

Figure 7 schematically depicts the 4 components and their relevant binding sites. Our model allows for all possible reactions between these basic components and their complexes, up until the formation of a full pseudodimer of the kind shown in Figure

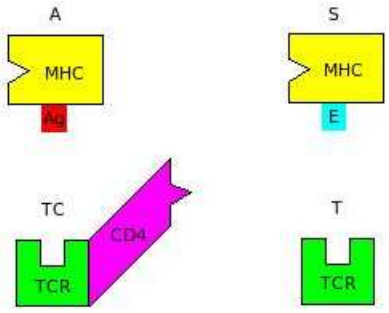

Figure 7: Basic components in our model. T-cell molecules are below, APC molecules above.

6. Once such a complex has been formed, we do not allow for further binding, as neither of the triggering models posits the formation of anything bigger. This results in a total of 30 possible chemical equations. In addition, we used a 2-compartment model, akin to those discussed in the Section 2, with a close-contact zone or synapse and the region outside it being the two compartments, and free diffusion between them being allowed. It is believed that the initial close-contact zones which form are much smaller than the eventual immunological synapse that results; as per Burroughs et al. (2006), who developed a mathematical description for the kinetic segregation model, these zones may only be about 100 nm in radius, and we have used the same size. Representing cross-compartment diffusion of the 4 basic components by chemical equations as well, we get a total of 34 reversible equations which comprise our model, given below:

$$A + T \overset{I}{\longleftrightarrow} AT \qquad TC + AT \overset{II}{\longleftrightarrow} TCAT$$
$$A + TCAT \overset{I}{\longleftrightarrow} ATCAT \qquad S + TCAT \overset{III}{\longleftrightarrow} STCAT$$
$$S + T \overset{III}{\longleftrightarrow} ST \qquad TC + ST \overset{II}{\longleftrightarrow} TCST$$
$$A + TCST \overset{I}{\longleftrightarrow} ATCST \qquad S + TCST \overset{III}{\longleftrightarrow} STCST$$
$$A + TC \overset{I}{\longleftrightarrow} ATC \qquad ATC + S \overset{II}{\longleftrightarrow} ATCS$$
$$ATC + ST \overset{II}{\longleftrightarrow} ATCST \qquad ATCS + T \overset{III}{\longleftrightarrow} ATCST$$
$$ATC + A \overset{II}{\longleftrightarrow} ATCA \qquad ATC + AT \overset{II}{\longleftrightarrow} ATCAT$$
$$ATCA + T \overset{I}{\longleftrightarrow} ATCAT \qquad S + TC \overset{III}{\longleftrightarrow} STC$$
$$STC + S \overset{II}{\longleftrightarrow} STCS \qquad STC + ST \overset{II}{\longleftrightarrow} STCST$$
$$STCS + T \overset{III}{\longleftrightarrow} STCST \qquad STC + A \overset{II}{\longleftrightarrow} STCA$$
$$STC + AT \overset{II}{\longleftrightarrow} STCAT \qquad STCA + T \overset{I}{\longleftrightarrow} STCAT$$
$$TC + A \overset{II}{\longleftrightarrow} TCA \qquad A + TCA \overset{I}{\longleftrightarrow} ATCA$$
$$S + TCA \overset{III}{\longleftrightarrow} STCA \qquad TCA + T \overset{I}{\longleftrightarrow} TCAT$$
$$TC + S \overset{II}{\longleftrightarrow} TCS \qquad A + TCS \overset{I}{\longleftrightarrow} ATCS$$
$$S + TCS \overset{III}{\longleftrightarrow} STCS \qquad TCS + T \overset{III}{\longleftrightarrow} TCST$$
$$T \overset{DT}{\longleftrightarrow} T_{out} \qquad A \overset{DA}{\longleftrightarrow} A_{out}$$
$$S \overset{DA}{\longleftrightarrow} S_{out} \qquad TC \overset{DT}{\longleftrightarrow} TC_{out}$$

Note that there are only five kinds of reactions happening here (in terms of rate constants): three types of binding reactions and two types of diffusion. These types, as denoted in the above equations, are detailed in Table 1, along with all the rate constants used. Also, we only allow for diffusion of the four basic components, as the assumption is that the complexes (which are formed trans-membrane) would break up if they went outside the close-contact zone. For the bivalent species TC, there are two possible binding sites for a pMHC (i.e., A or S): it can bind to the TCR or to the CD4. These are distinguished between in the equations above by the ordering of the letters: e.g., ATC denotes an agonist pMHC bound to the TCR of a TC, whereas TCA denotes CD4-MHC binding. All the different 5-letter species (viz. $ATCAT$, $STCAT$, $ATCST$, $STCST$) correspond to pseudodimers: in addition to the agonist-self kind shown in Figure 6, these can be also be agonist-agonist, self-agonist or self-self in theory.

Table 2 gives all other model parameters, including the initial values used for numbers of the basic species (these were assumed to be evenly distributed over the cell surfaces), as well as spatial parameters which were used for calculating concentrations and the diffusion rates given in Table 1. We used these parameters to encode the model in Matlab, and ran

Type	Description	k_{on}/k_{out}	k_{off}/k_{in}	Source
I	Binding of agonist pMHC to TCR	0.0055 $\mu m^2 s^{-1}$	0.01 s^{-1}	Burroughs et al. (2006)
II	Binding of MHC to CD4	0.0553 $\mu m^2 s^{-1}$	500 s^{-1}	Davis et al. (2003)
III	Binding of self pMHC to TCR	0.0055 $\mu m^2 s^{-1}$	3 s^{-1}	Burroughs et al. (2006)
DT	Diffusion on T-cell membrane	5.5609 s^{-1}	0.0015 s^{-1}	Computed as per Jansson et al. (2005)
DA	Diffusion on APC membrane	4.1679 s^{-1}	1.042x10^{-4} s^{-1}	"

Table 1: Different types of reaction and corresponding parameter values used.

Parameter	Description	Value	Source
T_{tot}	Total number of TCRs not bound to CD4	20,000	Estimate based on various experiments
A_{tot}	Total number of agonist pMHCs	200	"
S_{tot}	Total number of self pMHCs	50,000	"
TC_{tot}	Total number of TCRs bound to CD4	15,000	"
R_T	Radius of T-cell	3 μm	Jansson et al. (2005)
R_A	Radius of APC	10 μm	Jansson et al. (2005)
R_S	Radius of a close-contact zone	100 nm	Burroughs et al. (2006)
D	Diffusion coefficient	0.1 $\mu m^2 s^{-1}$	Jansson et al. (2005)

Table 2: Default parameter values used.

simulations using both mean-field Ordinary Differential Equations (ODEs), and Gillespie's Stochastic Simulation Algorithm (SSA) (Gillespie, 1977). The results follow.

3.3.1 Deterministic ODE simulation

The system of chemical equations was converted to ODEs assuming standard mass-action kinetics. These were integrated in Matlab (see Appendix A.4 for code) using the solver $ode15s$, over a time-span of 6 seconds: it has been shown that this amount of time is sufficient for TCR triggering to be caused following pMHC exposure (Huse et al., 2007). Initial values were set as per Table 2; we assumed the existence of 100 close-contact zones, as this approximated to a coverage of 30% (Burroughs et al., 2006) of an overall synapse of radius 2 μm (Jansson et al., 2005). However, simulation was carried out over just one zone (i.e., with a two-compartment model as described above) and the quantities of species obtained were multiplied by 100, since all zones are assumed to be of the same size.

Table 3 gives the numbers of complexes of different kinds obtained after 6 seconds; the results are depicted graphically in Figure 8. Note that since this is a continuous model, fractional numbers are possible, even though they are not physically meaningful. The numbers can be interpreted as the expected number of complexes which will have been formed on average, after 6 seconds of T cell-APC interaction. We see that the number for all possible kinds of pseudodimers are extremely small, which indicates that the chances of even a single one of these forming are minuscule. The number of single TCR-pMHC complexes seen is substantial, but the bulk of these are with self peptides. This is not surprising, since the number of self peptides on the APC is far greater (50,000 vs. 200 agonists), and this outweighs the 300-fold greater affinity assumed for agonist-TCR interactions (see Table 1). So whilst the pseudodimer hypothesis seems unlikely to be accurate based on these results, it is also unexplained how specificity in antigen recognition by the T cell could arise under a kinetic-segregation based triggering model.

3.3.2 Stochastic Gillespie simulation

Given that the number of agonists is very small, and also the tiny size of the close-contact zones, it is clear that stochastic effects (i.e., intrinsic noise) will play a major role in T cell-APC interaction. Also, lifetime differences between different kinds

TCR-Agonist	TCR-Self	Total Pseudodimers	ATCAT	STCAT	ATCST	STCST
3.53	69.56	0.045	10^{-4}	$2x10^{-3}$	$2x10^{-3}$	0.041

Table 3: Total numbers of complexes formed over 100 close-contact zones after 6 seconds of simulation using ODEs. 5-letter species refer to the different kinds of possible pseudodimers as per the system of equations given above.

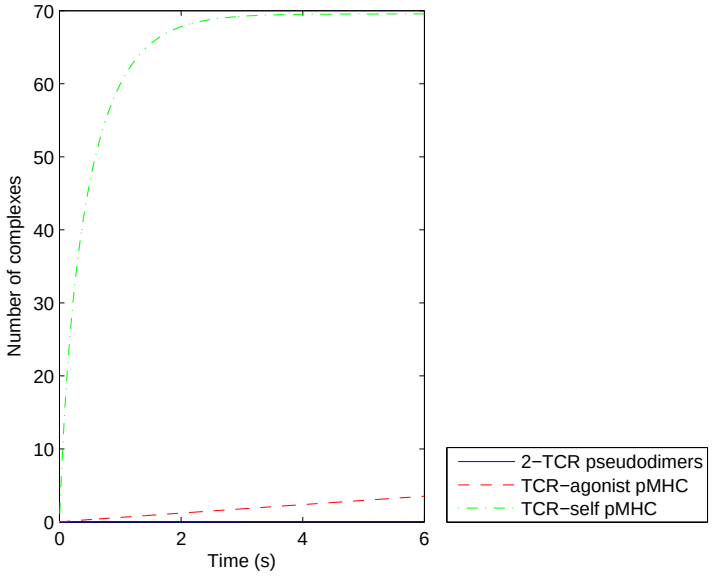

Figure 8: ODE simulation: quantities of different types of complexes.

	Cell 1			Cell 2			Cell 3		
	TCR-Ag	TCR-Se	Pseudodimers	TCR-Ag	TCR-Se	Pseudodimers	TCR-Ag	TCR-Se	Pseudodimers
Complexes	2	1,265	110	3	1,164	120	7	1,210	101
Mean life (s)	0.327	0.301	0.008	2.820	0.330	0.006	2.658	0.310	0.007
Std. dev. (s)	0.202	0.232	0.008	2.270	0.253	0.006	2.242	0.250	0.008
Max. life (s)	0.470	1.384	0.043	4.475	2.480	0.033	5.880	1.668	0.042

Table 4: Results of 3 independent stochastic simulations, each over 100 close-contact zones. Lifetime statistics were computed only within the 6 second simulation period, i.e. in effect all existing complexes at the end of that period were assumed to break down then. Ag and Se denote agonist and self peptide-MHCs respectively.

of complexes may be important (particularly in determining specificity), and a stochastic simulation can give us an idea of the distribution of lifetimes for any given species. Thus we also carried out simulation of our system of equations using the SSA (Gillespie, 1977). This is the standard algorithm for explicitly simulating discrete stochastic systems. It is essentially a Monte Carlo technique: it maintains a state vector of the number of molecules of different species in the system at each stage, and simulates just one reaction at a time. Each possible reaction is assigned a probability, which is directly proportional to its propensity function at that point in time. A uniform random number is then generated in order to choose which reaction to carry out next, and the state vector is updated accordingly. Another random number is generated to simulate the amount of time taken for this reaction to occur. This entire process is iterated through repeatedly, and after each reaction one may store the current state, so that at the end one has a complete history of the trajectory followed by the system.

There exist other methods for stochastic simulation, such as Stochastic Differential Equations (SDEs); but these are approximations which are used primarily because the explicit SSA is too slow for complicated systems. In our case, the Gillespie algorithm proved to be sufficiently fast: we tried using multiple kinds of implementations (Cao et al., 2004), and found the Direct Method (see Appendix A.5 for Matlab code) to be most efficient. This is what we used for the results reported here. All parameter values were kept the same as for the ODE simulations. Each close-contact zone was simulated independently, so 100 runs were carried out and their results summed up to get the numbers for the T cell as a whole. Also, rather than just looking at the final number of complexes after 6 seconds, all complexes formed and broken during that period were tracked, and their lifetimes were computed at a resolution of 10^{-4} seconds. Since the level of intrinsic noise may result in substantial variation over runs, we did the entire simulation 3 times to gauge the effect of this. The results are compiled in Table 4. Figure 9 illustrates the system's evolution for one of the 3 simulations.

The results show that in 2 simulations out of 3, TCR-agonist pMHC complexes, though formed in small numbers, are much more long-lived than TCR-self complexes, with an average lifetime difference of nearly 10-fold. This may help to account for the specificity of recognition under a model such as kinetic-segregation: if we assume, for instance, that a TCR needs to be held in the kinase-rich close-contact zone for at least 2.5-3 seconds before sufficient phosphorylation to cause triggering can occur, then it would seem that only agonist binding is likely to cause this to happen. The results of the first simulation indicate that the high level of intrinsic noise may mean that sometimes even TCR-agonist complexes do not last sufficiently long. However, the immune system may account for such noise by having a number of T cells or APCs for any given antigen, and thus a large enough number of cell-cell interactions to ensure that at least some result in activation. There is also uncertainty over the actual number of agonists on a typical APC; our figure of 200 may be an under-estimate, and the model of Burroughs et al. (2006), for instance, assumes an agonist density of 1 μm^{-2}, which corresponds to over 1000 altogether on the APC surface. Another factor to note is that specificity in T-cell activation possibly does not arise via TCR engagement alone; the process of costimulation discussed earlier may also play a role in preventing false alarms.

The second major observation from these results is that the pseudodimers formed are extremely short-lived, and out of more than 300 seen over all the runs, not a single one lasted for even 50 ms. Thus, as also noted from the ODE simulations, triggering based on pseudodimerization appears quite unlikely. Nearly all of the pseudodimers formed were of the self-self variety (this is seen in the ODE results in Table 3 as well), so agonist-specific triggering by this means seems particularly inviable.

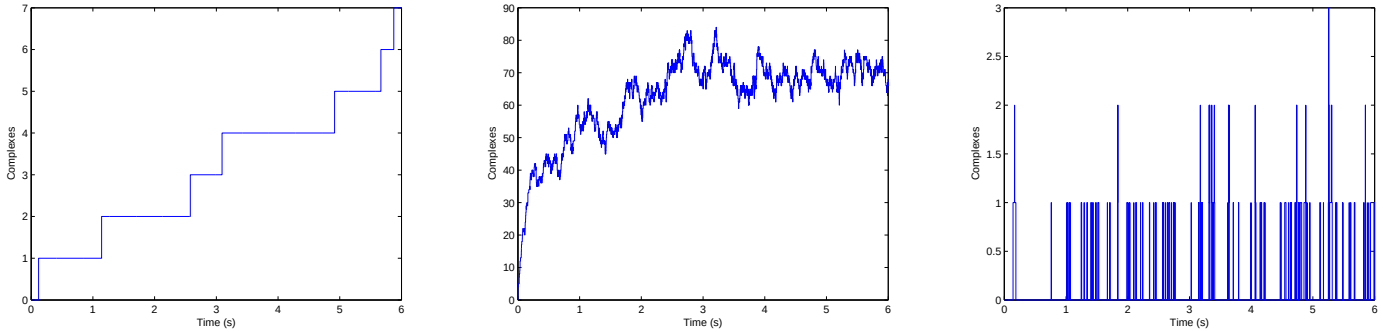

(a) TCR-agonist (b) TCR-self (c) Pseudodimers

Figure 9: Complex numbers for one stochastic simulation (Cell 3 in Table 4) over 6 seconds. Note the lifetime differences between the three types.

3.4 Discussion

We developed our model with the intention of seeing which theory of TCR triggering was better supported by the existing biochemical data. The results of both ODE and SSA simulations seem to indicate that there is little evidence to support the pseudodimerization idea. The key piece of data is the extremely low measured affinity between CD4 and MHC class II molecules: experiments have failed to detect any binding at concentrations of human soluble CD4 as high as 2 mM (Davis et al., 2003). This is reflected in our setting of the corresponding k_{off} value to 500 s^{-1} (see Table 1), which equates to a dissociation constant K_d of 5 mM. Thus, it would seem that this binding is too weak to permit stable pseudodimers to form; and as Figure 9(c) shows, in our simulations they break up virtually immediately. There are other issues with the theory as well: for instance, its effective assumption that a certain fraction of TCRs are pre-associated with CD4 (hence the species TC in our model). Irvine et al. (2002) base this on the fact that many TCRs are seen to be closely associated with CD4 molecules in *activated* T cells: this is clearly a logical flaw, as their theory is claiming that such associations are pre-requisites for triggering and activation to occur in the first place. The mechanism of association post- triggering is known, as CD4s are attached to Lck molecules, which can bind to phosphorylated ITAMs on the TCR-CD3 complex. However, there is no clear way for this to occur in a naïve T cell, and the authors do not propose any. Another problem is that of specificity; as mentioned previously, the vast majority of pseudodimers seen to form are self-self, and the few agonist containing ones that do form are also very short-lived, so there is apparently no way to mark them out. The authors mention the possibility of agonist binding causing a conformational change in CD4, but there seems to be no evidence for this.

From the point of view of the kinetic segregation model, the results from these simulations would appear to be compatible. The stochastic simulations show a significant difference between the average lifetimes of TCR-agonist and TCR-self complexes formed in close-contact zones, and thus provide a potential basis for specific recognition by T cells. There is substantial variation across the results of the 3 independent simulations carried out, particularly in terms of numbers and lifetimes of TCR-agonist complexes, indicating the high level of intrinsic noise in the system. Given more time, it would be advisable to run a larger number of simulations to generate more robust conclusions, including examining robustness to changes in model parameters and initial values. Nevertheless, the given results do clearly indicate that kinetic segregation is feasible. The theory does not provide a definitive reason for the importance of CD4 to sensitivity (Irvine et al., 2002), but it has been proposed that it may play a key role in amplifying the incipient signal generated by initial ITAM phosphorylation, subsequent to TCR-agonist binding (Davis et al., 2003).

4 Conclusions

In this project we looked at several different aspects of the process of T cell activation, approaching them from a mathematical modelling perspective. The first part consisted of implementing existing models and attempting to integrate them. However, the results did not seem to be of much benefit in terms of increasing our understanding of the system, because the activation model we were using as our framework (Bidot et al., 2008) was quite vague in terms of actual molecular mechanisms for different steps in the signaling pathway. So, in the second part, we focused on just TCR triggering, and attempted to develop a simple quantitative model to analyse the qualitative mechanisms already proposed. Using experimentally obtained data on binding affinities, diffusion rates and expression levels, we carried out simulations in a 2-compartment spatial framework of the chemical kinetics occurring at the T cell-APC interface. Our results appear to be helpful in virtually ruling out the pseudodimerization model, whilst providing support for a kinetic segregation based mechanism.

The model used by us is rather simple, and was developed with the pseudodimerization framework in mind; it may well be possible to modify it to better describe kinetic segregation, in particular incorporating the proposed role of CD4 as an amplifier acting post-triggering by an agonist (Davis et al., 2003). Also, a natural next step would be to extend the model to include the actual phosphorylation and downstream steps that are believed to occur inside the kinase-rich zones following TCR engagement; this has been looked at by Burroughs et al. (2006). The eventual goal would be to also account for the role of costimulation, bringing in the sort of framework discussed in Section 2.1 (Jansson et al., 2005), in order to provide a comprehensive quantitative description of how T cells are activated.

References

C. Bidot, F. Gruy, C.-S. Haudin, F. El Hentati, B. Guy, and C. Lambert. Mathematical modeling of T-cell activation kinetic. *Journal of Computational Biology*, 15(1):105–128, 2008.

Nigel J. Burroughs, Zorana Lazic, and P. Anton van der Merwe. Ligand detection and discrimination by spatial relocalization: A kinase-phosphatase segregation model of TCR activaton. *Biophysical Journal*, 91(5):1619–1629, 2006.

Yang Cao, Hong Li, and Linda Petzold. Efficient formulation of the stochastic simulation algorithm for chemically reacting systems. *The Journal of Chemical Physics*, 121(9):4059–4067, 2004.

Simon J. Davis and P. Anton van der Merwe. The kinetic-segregation model: TCR triggering and beyond. *Nature Immunology*, 7(8):803–809, 2006.

Simon J. Davis and P. Anton van der Merwe. The structure and ligand interactions of CD2: implications for T-cell function. *Immunology Today*, 17(4):177–187, 1996.

Simon J. Davis, Shinji Ikemizu, Edward J. Evans, Lars Fugger, Talitha R. Bakker, and P. Anton van der Merwe. The nature of molecular recognition by T cells. *Nature Immunology*, 4(3):217–224, 2003.

Daniel T. Gillespie. Exact stochastic simulation of coupled chemical reactions. *The Journal of Physical Chemistry*, 81(25): 2340–2361, 1977.

Morgan Huse, Lawrence O. Klein, Andrew T. Girvin, Joycelyn M. Faraj, Qi-Jing Li, Michael S. Kuhns, and Mark M. Davis. Spatial and temporal dynamics of T cell receptor signaling with a photoactivatable agonist. *Immunity*, 27(1):76–88, 2007.

Darrell J. Irvine, Marco A. Purbhoo, Michelle Krogsgaard, and Mark M. Davis. Direct observation of ligand recognition by T cells. *Nature*, 419(6909):845–849, 2002.

Andreas Jansson, Eleanor Barnes, Paul Klenerman, Mikael Harlén, Poul Sørensen, Simon J. Davis, and Patric Nilsson. A theoretical framework for quantitative analysis of the molecular basis of costimulation. *The Journal of Immunology*, 175(3): 1575–1585, 2005.

Michelle Krogsgaard and Mark M. Davis. How T cells 'see' antigen. *Nature Immunology*, 6(3):239–245, 2005.

Kenneth Murphy, Paul Travers, and Mark Walport. *Janeway's Immunobiology (Seventh Edition)*. Garland Science, 2008.

A Matlab Code

A.1 Costimulation model code

```
function dy = diff2(t,y)
    km = (size(y,1)-14)/3;

    aB = 7.07;
    as = 12.6;
    iCD28=14;
    iB71=0.64;
    iB72=13.7;

    k28 = 3.6e-2;
    g28 = 1e-3;
    lambda = 7.7e-3;
    kB = 0;
    gB = 0;
    kDC = 2.7e-2;
    gDC = 2.7e-4;

    a1=0.77;
    a2=0.22;
    a3=1.09;
    a4=1.19;
    a22=0.22;
    a33=0.13;
    a44=0.17;
    d1=28;
    d2=1.6;
    d3=5.1;
    d4=0.43;
    d22=1.6;
    d33=0.052;
    d44=0.0044;

    dCD28 = y(2)+y(11)+2*y(12)+y(10);
    fCD28 = (dCD28-iCD28)/dCD28;
    dB72 = y(9)+y(10)+y(13)+2*y(14);
    fB72 = (dB72-iB72)/dB72;
    dB71 = y(7)+y(11)+y(12);

    dy = zeros(size(y));
    dy(10) = a1*y(2)*y(9) - d1*y(10);
    dy(11) = a2*y(2)*y(7) - d2*y(11) - a22*y(2)*y(11) + d22*y(12);
    dy(12) = a22*y(2)*y(11) - d22*y(12);
    dy(13) = a3*y(5)*y(9) - d3*y(13) - a33*y(13)*y(9) + d33*y(14);
```

```
    dy(14) = a33*y(13)*y(9) - d33*y(14);
    dy(17) = a4*y(5)*y(7) - d4*y(17) - a44*y(5)*y(17) - a44*y(7)*y(17) + d44*y(15) + d44*y(16);
    SBk=0;
    SCk=0;
    SEk=0;
    for k=1:km
        Bk = 12+3*k;
        Ck = Bk+1;
        Ek = Ck+1;
        Bk1 = Ek+1;
        Ck1 = Bk1+1;
        Ek1 = Ck1+1;
        dy(Bk) = -a44*y(5)*y(Bk) - d44*y(Bk) + a44*y(7)*y(Ek);
        dy(Ck) = -a44*y(7)*y(Ck) - d44*y(Ck) + a44*y(5)*y(Ek);
        if(k<km)
            dy(Bk) = dy(Bk) + d44/2*y(Ek1);
            dy(Ck) = dy(Ck) + d44/2*y(Ek1);
            dy(Ek1) = a44*y(5)*y(Bk) + a44*y(7)*y(Ck) - a44*y(7)*y(Ek1) - a44*y(5)*y(Ek1)...
                      - d44*y(Ek1) + d44*y(Bk1) + d44*y(Ck1);
        end
        dB71 = dB71+(k+1)*y(Bk)+k*(y(Ck)+y(Ek));
        SBk = SBk+y(Bk);
        SCk = SCk+y(Ck);
        SEk = SEk+y(Ek);
        dy(6) = dy(6)-((k+1)*dy(Bk)+k*(dy(Ck)+dy(Ek)))*as;
        dy(4) = dy(4)-((k+1)*dy(Ck)+k*(dy(Bk)+dy(Ek)))*as;
    end
    fB71 = (dB71-iB71)/dB71;

    dy(3) = kB*as/aB*y(5) - gB*y(3);
    dy(2) = -a1*y(2)*y(9) - a2*y(2)*y(7) - a22*y(2)*y(11) + d1*y(10) + d2*y(11)...
            + d22*y(12) + g28/as*y(1) - k28*fCD28*y(2);
    dy(5) = -a3*y(5)*y(9) - a4*y(5)*y(7) - a44*y(5)*(SEk+SBk) + d3*y(13) + d4*y(17)...
            + d44*(SCk + (SEk-y(17))/2) + lambda/as*y(4) + gB*aB/as*y(3) - kB*y(5);
    dy(7) = -a2*y(2)*y(7) - a4*y(5)*y(7) - a44*y(7)*(SEk+SCk) + d2*y(11) + d4*y(17)...
            + d44*(SBk + (SEk-y(17))/2) + gDC/as*y(6) - kDC*fB71*y(7);
    dy(9) = -a1*y(2)*y(9) - a3*y(5)*y(9) - a33*y(13)*y(9) + d1*y(10) + d3*y(13)...
            + d33*y(14) + gDC/as*y(8) - kDC*fB72*y(9);
    dy(1) = (-dy(2)-dy(11)-2*dy(12)-dy(10))*as;
    dy(6) = dy(6) + (-dy(7)-dy(11)-dy(12))*as;
    dy(8) = (-dy(9)-dy(10)-dy(13)-2*dy(14))*as;
    dy(4) = dy(4) + (-dy(5)-dy(13)-dy(14))*as - dy(3)*aB;
end

clear all;

as = 12.6;
iCD28=14;
iB71=0.64;
iB72=13.7;
```

```
tCD28tot = 9.2e3;
tCTLAtot = 0.4e3;
dB71tot = 2e3;
dB72tot = 43e3;
mCD28 = 0.3;
mCTLA = 1;
mB71 = 0.6;
mB72 = 0.6;

km = 25;
y0 = zeros(14+3*km,1);
y0(1:9) = [tCD28tot*mCD28, iCD28, 0, tCTLAtot*mCTLA, 0, dB71tot*mB71, iB71, dB72tot*mB72, iB72];
tspan = 0:5400;

[T Y] = ode15s(@diff2,tspan,y0);
plot(T,as*Y(:,10));
hold on;
plot(T,as*(Y(:,11)+2*Y(:,12)),'--r');
plot(T,as*(Y(:,13)+Y(:,14)),':k');
c4b1=0;
for k=1:km
    c4b1 = c4b1+as*((k+1)*Y(:,13+3*k)+k*(Y(:,12+3*k)+Y(:,14+3*k)));
end
plot(T,c4b1,'-.g');
xlabel('Time (s)');
ylabel('Number of complexed CD28/CTLA-4');
legend('CD28:B72','CD28:B71','CTLA4:B72','CTLA4:B71','Location','NorthEastOutside');
```

A.2 Activation model code

```
function dy = diffy(t,y)
    bulk=1.8e-16;
    ov=1e-12;
    area=1.5e-10;
    syn=0.2*area;
    osyn=area-syn;
    NA=6.023e23;
    koncf=1e6/3;

    phi=9.16e-5;
    lambda=syn/osyn;
    CD48=75000/NA/area;
    CD69L=CD48/800;
    CD80=CD48/8;
    k1=60;
    kv1=k1*syn/bulk;
    k2=k1;
    kv2=k2*osyn/bulk;
    ka1=0.057;
```

```
kd1=1e-3;
kd2=kd1;
kd3=kd1;
kd4=kd1;
ke1=1e-3;
ke2=ke1;
ke3=kd3;
ke4=ke3;
ke5=ke3;
kf2=0.01;
kf3=0.015;
kf4=0.015;
kf5=150;
kef5=kf5*area/ov;
kvf5=kf5*area/bulk;
ki1=1.56e-3;
kvi1=ki1*syn/bulk;
ki2=ki1;
kvi2=kvi1;
ki3=ki1;
kvi3=kvi1;
ki4=ki1;
kvi4=ki4*area/bulk;
km1=1e-4;
ksm1=km1*bulk/syn;
km2=1e-4;
ksm2=km2*bulk/area;
km3=1e-4;
kem3=km3*bulk/ov;
koffCD28=1.6;
koffCD48=0.05;
koffCD69=0.01;
koffIL2m=0.035;
keoffIL2m=koffIL2m*area/ov;
koffIL2s=0.035;
koffTL=ka1;
konCD28=6.6e5*koncf;
konCD48=1200*koncf;
konCD69=7e3*koncf;
konIL2m=1.06e3;
keonIL2m=konIL2m*area/ov;
konIL2s=1.06e3;
konTL=900*koncf;
kpp1=5e-10;
kvpp1=kpp1*syn/bulk;
kpp2=5e-10;
kvpp2=kpp2*area/bulk;
kpp3=5e-4;
kvpp3=kpp3*ov/bulk;
kp1=760;
```

```
    ksp1=kp1*bulk/syn;
    kp2=940;
    ksp2=kp2*bulk/area;
    kp3=0.019;
    kep3=kp3*bulk/ov;
    L=1000/NA/(8*area);
    s=1.83e-5;
    sp=0;
    Smax=40000/NA/area;
    Tmax=Smax;
    CD28hsmax=Smax/20;
    CD28max=CD28hsmax;

    dy=zeros(22,1);
    dy(1) = -konTL*L*y(1) + koffTL*y(3) + s*(Tmax-y(1)) + phi*(y(2)-y(1)) + k1*y(22)*(Tmax-y(1));
    dy(2) = s*(Smax-y(2)) - lambda*phi*(y(2)-y(1)) + k2*y(22)*(Smax-y(2));
    dy(3) = konTL*L*y(1) - koffTL*y(3) - konCD48*y(3)*CD48 + koffCD48*y(4);
    dy(4) = konCD48*y(3)*CD48 - koffCD48*y(4) - ka1*y(4);
    dy(5) = ka1*y(4) - ki1*y(5);
    dy(6) = kvi1*y(5) - (kp1+kp2)*y(6)*y(11) - (km1+km2+km3)*y(6) - kd1*y(6);
    dy(7) = sp*(CD28hsmax - y(7)) - lambda*phi*(y(7)-y(8));
    dy(8) = phi*(y(7)-y(8)) - konCD28*y(8)*CD80 + koffCD28*y(9) + sp*(CD28max-y(8));
    dy(9) = konCD28*y(8)*CD80 - koffCD28*y(9) - kf2*y(9);
    dy(10) = kf2*y(9) - ki2*y(10);
    dy(11) = kvi2*y(10) - (kp1+kp2)*y(6)*y(11) - kd2*y(11);
    dy(12) = ksm1*y(6) + ksp1*y(6)*y(11) + kpp1*y(22) - konCD69*y(12)*CD69L + koffCD69*y(13) - ke1*y(12);
    dy(13) = konCD69*y(12)*CD69L - koffCD69*y(13) - kf3*y(13);
    dy(14) = kf3*y(13) - ki3*y(14);
    dy(15) = kvi3*y(14) - kp3*y(15) - kd3*y(15);
    dy(16) = ksm2*y(6) + ksp2*y(6)*y(11) + kpp2*y(22) - konIL2m*y(18)*y(16) + koffIL2m*y(20) - kf5*y(16)*y(22)...
             - ke2*y(16);
    dy(17) = -konIL2s*y(18)*y(17) + koffIL2s*y(19) + kef5*y(16)*y(22) - ke3*y(17);
    dy(18) = kep3*y(15) + kem3*y(6) + kpp3*y(22) - konIL2s*y(18)*y(17) + koffIL2s*y(19) - keonIL2m*y(18)*y(16)...
             + keoffIL2m*y(20) - ke4*y(18);
    dy(19) = konIL2s*y(18)*y(17) - koffIL2s*y(19) - ke5*y(19);
    dy(20) = -kf4*y(20) + konIL2m*y(18)*y(16) - koffIL2m*y(20);
    dy(21) = kf4*y(20) - ki4*y(21);
    dy(22) = kvi4*y(21) - kvf5*y(16)*y(22) - kv1*y(22)*(Tmax-y(1)) - (kvpp1 + kvpp2 + kvpp3 +kd4)*y(22)...
             - kv2*y(22)*(Smax-y(2));
end

tspan=0:18000;
y0=[3.25e-10 3.25e-10 0 0 0 0 1.625e-11 1.625e-11 0 0 0 0 0 0 0 0 0 0 0 0 0 0];
[T Y] = ode15s(@diffy,tspan,y0);
CD3 = Y(:,1)+sum(Y(:,3:5),2);
CD28 = sum(Y(:,8:10),2);
CD69 = sum(Y(:,12:14),2);
IL2RM = Y(:,16)+sum(Y(:,20:21),2);
figure;
plot(T,CD3);
```

```
hold on;
plot(T,CD28*10,'--r');
plot(T,CD69*100,':k');
plot(T,IL2RM*100,'-.g');
legend('TCR','CD28(x10)','CD69(x100)','IL2 receptor(x100)','Location','NorthEast');
xlabel('Time (s)');
ylabel('Concentration (mol/m^2)');
figure;
plot(T,Y(:,22));
legend('IL2-IL2 receptor complexes','Location','NorthEast');
xlabel('Time (s)');
ylabel('Concentration (mol/m^3)');
```

A.3 Integrated model code

```
function dy = diffc(t,y)
    km = (size(y,1)-38)/3;

    % Micrometric value of synapse area for Jansson
    as=12.6;

    % Area/volume parameters for Bidot, in metric units
    bulk=9.048e-16;
    ov=1e-12;
    area=4.524e-10;
    syn=as*1e-12;
    osyn=area-syn;

    NA=6.023e23;
    koncf=1e6/3;

    iCD28=14;
    iB71=0.64;
    iB72=13.7;

    k28 = 3.6e-2;
    g28 = 1e-3;
    kDC = 2.7e-2;
    gDC = 2.7e-4;

    a1=0.77;
    a2=0.22;
    a3=1.09;
    a4=1.19;
    a22=0.22;
    a33=0.13;
    a44=0.17;
    d1=28;
    d2=1.6;
    d3=5.1;
```

```
d4=0.43;
d22=1.6;
d33=0.052;
d44=0.0044;

dCD28 = y(2)+y(11)+2*y(12)+y(10);
fCD28 = (dCD28-iCD28)/dCD28;
dB72 = y(9)+y(10)+y(13)+2*y(14);
fB72 = (dB72-iB72)/dB72;
dB71 = y(7)+y(11)+y(12);

% Bidot et al. model parameters
phi=9.16e-5;
lambda=syn/osyn;
CD48=75000/NA/area;
CD69L=CD48/300;
k1=60;
kv1=k1*syn/bulk;
k2=k1;
kv2=k2*osyn/bulk;
ka1=0.057;
kd1=1e-3;
kd2=kd1;
kd3=kd1;
kd4=kd1;
ke1=1e-3;
ke2=ke1;
ke3=kd3;
ke4=ke3;
ke5=ke3;
kf2=0.01;
kf3=0.015;
kf4=0.015;
kf5=150;
kef5=kf5*area/ov;
kvf5=kf5*area/bulk;
ki1=1.56e-3;
kvi1=ki1*syn/bulk;
ki2=ki1;
kvi2=kvi1;
ki3=ki1;
kvi3=kvi1;
ki4=ki1;
kvi4=ki4*area/bulk;
km1=1e-4;
ksm1=km1*bulk/syn;
km2=1e-4;
ksm2=km2*bulk/area;
km3=1e-4;
kem3=km3*bulk/ov;
```

```
koffCD48=0.05;
koffCD69=0.01;
koffIL2m=0.035;
keoffIL2m=koffIL2m*area/ov;
koffIL2s=0.035;
koffTL=ka1;
konCD48=1200*koncf;
konCD69=7e3*koncf;
konIL2m=1.06e3;
keonIL2m=konIL2m*area/ov;
konIL2s=1.06e3;
konTL=900*koncf;
kpp1=5e-10;
kvpp1=kpp1*syn/bulk;
kpp2=5e-10;
kvpp2=kpp2*area/bulk;
kpp3=5e-4;
kvpp3=kpp3*ov/bulk;
kp1=760;
ksp1=kp1*bulk/syn;
kp2=940;
ksp2=kp2*bulk/area;
kp3=0.019;
kep3=kp3*bulk/ov;
L=1000/NA/(3*area);
s=1.83e-5;
Smax=40000/NA/area;
Tmax=Smax;

dy = zeros(size(y));
dy(10) = a1*y(2)*y(9) - d1*y(10);
dy(11) = a2*y(2)*y(7) - d2*y(11) - a22*y(2)*y(11) + d22*y(12);
dy(12) = a22*y(2)*y(11) - d22*y(12);
dy(13) = a3*y(5)*y(9) - d3*y(13) - a33*y(13)*y(9) + d33*y(14);
dy(14) = a33*y(13)*y(9) - d33*y(14);
dy(17) = a4*y(5)*y(7) - d4*y(17) - a44*y(5)*y(17) - a44*y(7)*y(17) + d44*y(15) + d44*y(16);
SBk=0;
SCk=0;
SEk=0;
CTLA4c=y(13)+y(14);
for k=1:km
    Bk = 12+3*k;
    Ck = Bk+1;
    Ek = Ck+1;
    Bk1 = Ek+1;
    Ck1 = Bk1+1;
    Ek1 = Ck1+1;
    dy(Bk) = -a44*y(5)*y(Bk) - d44*y(Bk) + a44*y(7)*y(Ek);
    dy(Ck) = -a44*y(7)*y(Ck) - d44*y(Ck) + a44*y(5)*y(Ek);
    if(k<km)
```

```
        dy(Bk) = dy(Bk) + d44/2*y(Ek1);
        dy(Ck) = dy(Ck) + d44/2*y(Ek1);
        dy(Ek1) = a44*y(5)*y(Bk) + a44*y(7)*y(Ck) - a44*y(7)*y(Ek1) - a44*y(5)*y(Ek1) - d44*y(Ek1)...
                  + d44*y(Bk1) + d44*y(Ck1);
    end
    dB71 = dB71+(k+1)*y(Bk)+k*(y(Ck)+y(Ek));
    CTLA4c = CTLA4c+(k+1)*y(Ck)+k*(y(Bk)+y(Ek));
    SBk = SBk+y(Bk);
    SCk = SCk+y(Ck);
    SEk = SEk+y(Ek);
    dy(6) = dy(6)-((k+1)*dy(Bk)+k*(dy(Ck)+dy(Ek)))*as;
    dy(4) = dy(4)-((k+1)*dy(Ck)+k*(dy(Bk)+dy(Ek)))*as;
end
fB71 = (dB71-iB71)/dB71;
dy(2) = -a1*y(2)*y(9) - a2*y(2)*y(7) - a22*y(2)*y(11) + d1*y(10) + d2*y(11) + d22*y(12) + g28/as*y(1)...
        - k28*fCD28*y(2);
dy(5) = -a3*y(5)*y(9) - a4*y(5)*y(7) - a44*y(5)*(SEk+SBk) + d3*y(13) + d4*y(17) + d44*(SCk + (SEk-y(17))/2)...
        + lambda/as*y(4);
dy(7) = -a2*y(2)*y(7) - a4*y(5)*y(7) - a44*y(7)*(SEk+SCk) + d2*y(11) + d4*y(17) + d44*(SBk + (SEk-y(17))/2)...
        + gDC/as*y(6) - kDC*fB71*y(7);
dy(9) = -a1*y(2)*y(9) - a3*y(5)*y(9) - a33*y(13)*y(9) + d1*y(10) + d3*y(13) + d33*y(14) + gDC/as*y(8)...
        - kDC*fB72*y(9);
dy(1) = (-dy(2)-dy(11)-2*dy(12)-dy(10))*as;
dy(6) = dy(6) + (-dy(7)-dy(11)-dy(12))*as;
dy(8) = (-dy(9)-dy(10)-dy(13)-2*dy(14))*as;
dy(4) = dy(4) + (-dy(5)-dy(13)-dy(14))*as;

% Bidot eqns.
y2 = y(15+3*km:size(y,1));
dy2 = zeros(24,1);
dy2(1) = -konTL*L*y2(1) + koffTL*y2(3) + s*(Tmax-y2(1)) + phi*(y2(2)-y2(1)) + k1*y2(22)*(Tmax-y2(1));
dy2(2) = s*(Smax-y2(2)) - lambda*phi*(y2(2)-y2(1)) + k2*y2(22)*(Smax-y2(2));
dy2(3) = konTL*L*y2(1) - koffTL*y2(3) - konCD48*y2(3)*CD48 + koffCD48*y2(4);
dy2(4) = konCD48*y2(3)*CD48 - koffCD48*y2(4) - ka1*y2(4);
dy2(5) = ka1*y2(4) - ki1*y2(5);
dy2(6) = kvi1*y2(5) - (kp1+kp2)*y2(6)*(y2(11)+y2(24)) - (km1+km2+km3)*y2(6) - kd1*y2(6);
dy2(7) = dy(1)/NA/osyn;
dy2(8) = dy(2)*1e12/NA;
dy2(9) = (dy(10)+dy(11)+2*dy(12))*1e12/NA;
dy2(10) = kf2*y2(9) - ki2*y2(10);
dy2(11) = kvi2*y2(10) - (kp1+kp2)*y2(6)*y2(11) - kd2*y2(11);
dy2(12) = ksm1*y2(6) + ksp1*y2(6)*y2(11) + kpp1*y2(22) - konCD69*y2(12)*CD69L + koffCD69*y2(13) - ke1*y2(12);
dy2(13) = konCD69*y2(12)*CD69L - koffCD69*y2(13) - kf3*y2(13);
dy2(14) = kf3*y2(13) - ki3*y2(14);
dy2(15) = kvi3*y2(14) - kp3*y2(15) - kd3*y2(15);
dy2(16) = ksm2*y2(6) + ksp2*y2(6)*y2(11) + kpp2*y2(22) - konIL2m*y2(18)*y2(16) + koffIL2m*y2(20)...
          - kf5*y2(16)*y2(22) - ke2*y2(16);
dy2(17) = -konIL2s*y2(18)*y2(17) + koffIL2s*y2(19) + kef5*y2(16)*y2(22) - ke3*y2(17);
dy2(18) = kep3*y2(15) + kem3*y2(6) + kpp3*y2(22) - konIL2s*y2(18)*y2(17) + koffIL2s*y2(19)...
          - keonIL2m*y2(18)*y2(16) + keoffIL2m*y2(20) - ke4*y2(18);
```

```
    dy2(19) = konIL2s*y2(18)*y2(17) - koffIL2s*y2(19) - ke5*y2(19);
    dy2(20) = -kf4*y2(20) + konIL2m*y2(18)*y2(16) - koffIL2m*y2(20);
    dy2(21) = kf4*y2(20) - ki4*y2(21);
    dy2(22) = kvi4*y2(21) - kvf5*y2(16)*y2(22) - kv1*y2(22)*(Tmax-y2(1)) - (kvpp1 + kvpp2 + kvpp3 +kd4)*y2(22)...
              - kv2*y2(22)*(Smax-y2(2));
    dy2(23) = kf2*CTLA4c*1e12/NA - ki2*y2(23);
    dy2(24) = kvi2*y2(23) - (kp1+kp2)*y2(6)*y2(24) - kd2*y2(24);

    dy(15+3*km:size(dy,1)) = dy2;
end

tspan=0:18000;

aB = 439.8;
as = 12.6;

iCD28=14;
iB71=0.64;
iB72=13.7;

tCD28tot = 9.2e3;
tCTLAtot = 0.4e3;
dB71tot = 2e3;
dB72tot = 43e3;
mCD28 = 0.3;
mCTLA = 1;
mB71 = 0.6;
mB72 = 0.6;

km = 25;
y0 = zeros(38+3*km,1);
y0(1:9) = [tCD28tot*mCD28, iCD28, 0, tCTLAtot*mCTLA, 0, dB71tot*mB71, iB71, dB72tot*mB72, iB72];
y0(15+3*km)=3.25e-10;
y0(16+3*km)=3.25e-10;
y0(21+3*km)=y0(1)/(6.023e11*aB);
y0(22+3*km)=y0(2)/6.023e11;

[T Y] = ode15s(@diffc,tspan,y0);

figure;
plot(T,as*Y(:,10));
hold on;
plot(T,as*(Y(:,11)+2*Y(:,12)),'r');
plot(T,as*(Y(:,13)+Y(:,14)),'k');
c4b1=0;
for k=1:km
    c4b1 = c4b1+as*((k+1)*Y(:,13+3*k)+k*(Y(:,12+3*k)+Y(:,14+3*k)));
end
plot(T,c4b1,'g');
legend('CD28:B72','CD28:B71','CTLA4:B72','CTLA4:B71','Location','NorthEastOutside');
```

```
% Bidot
CD3 = Y(:,15+km*3)+sum(Y(:,17+km*3:19+km*3),2);
CD28 = sum(Y(:,22+km*3:24+km*3),2);
CD69 = sum(Y(:,26+km*3:28+km*3),2);
IL2RM = Y(:,30+km*3)+sum(Y(:,34+km*3:35+km*3),2);
CTLA4 = Y(:,37+km*3)+(Y(:,5)+Y(:,13)+Y(:,14)+c4b1)/6.023e11;
figure;
plot(T,CD3);
hold on;
plot(T,CD28,'--r');
plot(T,CD69*100,':k');
plot(T,IL2RM*1000,'-.g');
plot(T,CTLA4/10,'oy');
legend('TCR','CD28','CD69(x100)','IL2 receptor(x1000)','CTLA-4(x0.1)','Location','NorthEast');
xlabel('Time (s)');
ylabel('Concentration (mol/m^2)');
figure;
plot(T,Y(:,36+km*3));
legend('IL2-IL2 receptor complexes');
xlabel('Time (s)');
ylabel('Concentration (mol/m^3)');
```

A.4 ODE code for our model

```
function dy = diff3(t,y)

        rT=3;
        rD=10;
        rS=0.1;
        areaT = 4*pi*rT^2;
        areaD = 4*pi*rD^2;
        areaS = pi*rS^2;
        D=0.1;
        thT=rS/rT;
        thD=rS/rD;

        gT = D/rT^2*(1+cos(thT))/(2*log(2/(1-cos(thT))) - (1+cos(thT)));
        gD = D/rD^2*(1+cos(thD))/(2*log(2/(1-cos(thD))) - (1+cos(thD)));
        kT = gT*(areaT-areaS)/areaS;
        kD = gD*(areaD-areaS)/areaS;

        n1 = 0.0055;
        n2 = 0.0553;
        n3 = n1;
        f1 = 1e-2;
        f2 = 5e2;
        f3 = 3;
        T = y(17);
        A = y(18);
```

```
        S = y(19);
        C = y(20);

        dy = zeros(24,1);
        dy(1) = n1*T*A - f1*y(1) - n2*y(1)*(C+y(8)+y(11)) + f2*(y(2)+y(3)+y(4));
        dy(2) = n2*y(1)*C - f2*y(2) + n1*(y(14)*T - y(2)*A) -f1*(y(2) - y(3)) - n3*y(2)*S + f3*y(4);
        dy(3) = n1*(y(2)*A + y(10)*T) + n2*y(8)*y(1) - (2*f1 + f2)*y(3);
        dy(4) = n3*y(2)*S + n2*y(11)*y(1) + n1*y(13)*T - (f1+f2+f3)*y(4);
        dy(5) = n3*T*S - f3*y(5) - n2*y(5)*(C+y(8)+y(11)) + f2*(y(6)+y(16)+y(7));
        dy(6) = n2*y(5)*C - f2*y(6) - n1*y(6)*A + n3*(y(15)*T-y(6)*S) + f1*y(16) + f3*(y(7) - y(6));
        dy(7) = n3*(y(6)*S + y(12)*T) + n2*y(11)*y(5) - (2*f3+f2)*y(7);
        dy(8) = n1*C*A - f1*y(8) -n2*y(8)*(S+y(5)+A+y(1)) + f2*(y(9)+y(16)+y(10)+y(3));
        dy(9) = n2*y(8)*S - (f1+f2)*y(9) - n3*y(9)*T + f3*y(16) + n1*y(15)*A;
        dy(10) = n2*y(8)*A - f2*y(10) + n1*(y(14)*A - y(10)*T) - f1*(y(10) - y(3));
        dy(11) = n3*C*S - f3*y(11) - n2*y(11)*(S+y(5)+A+y(1)) + f2*(y(12)+y(7)+y(13)+y(4));
        dy(12) = n2*y(11)*S + n3*(y(15)*S - y(12)*T) - y(12)*(f2+f3) + f3*y(7);
        dy(13) = n2*y(11)*A + n3*y(14)*S - y(13)*(f2+f3) - n1*y(13)*T + f1*y(4);
        dy(14) = n2*C*A - f2*y(14) - n1*y(14)*(A+T) - n3*y(14)*S + f1*(y(10)+y(2)) + f3*y(13);
        dy(15) = n2*C*S - f2*y(15) - n1*y(15)*A - n3*y(15)*(S+T) + f1*y(9) + f3*(y(12)+y(6));
        dy(16) = n1*y(6)*A + n2*y(8)*y(5) + n3*y(9)*T - (f1+f2+f3)*y(16);
        dy(17) = -n1*T*(A+y(10)+y(13)+y(14)) - n3*T*(S+y(9)+y(12)+y(15)) + f1*(y(1)+y(3)+y(4)+y(2))...
                 + f3*(y(5)+y(16)+y(7)+y(6)) + gT*y(21)/areaS - kT*T;
        dy(18) = -n1*A*(T+y(2)+y(6)+C+y(14)+y(15)) - n2*A*(y(8)+y(11)+C) + f1*(y(1)+y(3)+y(16)+y(8)+y(10)+y(9))...
                 + f2*(y(10)+y(13)+y(14)) + gD*y(22)/areaS - kD*A;
        dy(19) = -n3*S*(y(2)+T+y(6)+C+y(14)+y(15)) - n2*S*(y(8)+y(11)+C) + f3*(y(4)+y(5)+y(7)+y(11)+y(13)+y(12))...
                 + f2*(y(9)+y(12)+y(15)) + gD*y(23)/areaS - kD*S;
        dy(20) = -n2*C*(y(1)+y(5)+A+S) - n1*A*C - n3*S*C + f2*(y(2)+y(6)+y(14)+y(15)) + f1*y(8) + f3*y(11)...
                 + gT*y(24)/areaS - kT*C;
        dy(21) = -gT*y(21) + kT*T*areaS;
        dy(22) = -gD*y(22) + kD*A*areaS;
        dy(23) = -gD*y(23) + kD*S*areaS;
        dy(24) = -gT*y(24) + kT*C*areaS;
end

rT=3;
rD=10;
rS=0.1;
areaS = pi*rS^2;
areaT = 4*pi*rT^2;
areaD = 4*pi*rD^2;

y0 = zeros(24,1);
y0(17:20) = [20000/areaT; 200/areaD; 50000/areaD; 15000/areaT];
y0(21:24) = [20000-100*areaS*y0(17); 200-100*areaS*y0(18); 50000-100*areaS*y0(19); 15000-100*areaS*y0(20)];

tspan = 0:0.0001:6;

[T Y] = ode15s(@diff3, tspan, y0);
Y = Y*areaS;
```

```
c5 = Y(:,3)+Y(:,4)+Y(:,7)+Y(:,16);
ag = sum(Y(:,1:4),2)+Y(:,3)+sum(Y(:,8:10),2)+Y(:,16);
se = sum(Y(:,4:7),2)+Y(:,7)+sum(Y(:,11:13),2)+Y(:,16);

figure;
plot(T,c5*100);
hold on;
plot(T,ag*100,'--r');
plot(T,se*100,'-.g');
legend('2-TCR pseudodimers','TCR-agonist pMHC','TCR-self pMHC', 'Location','SouthEastOutside');
xlabel('Time (s)');
ylabel('Number of complexes');
```

A.5 SSA code for our model

```
function Y = dgtcr(Tmax)

    V = [ 1 -1  0  0  0  0  0  0  0  0  0  0  0 -1  0  0  0  0  0  0 -1  0  0  0  0  0  0  0  0  0  0  0  0  0;
          0  1 -1 -1  0  0  0  0  0  0  0  0  0  0  0  0  0  0  0  0  0  0  0  0  0  1  0  0  0  0  0  0  0  0;
          0  0  1  0  0  0  0  0  0  0  0  0  0  1  1  0  0  0  0  0  0  0  0  0  0  0  0  0  0  0  0  0  0  0;
          0  0  0  1  0  0  0  0  0  0  0  0  0  0  0  0  0  0  0  0  1  1  0  0  0  0  0  0  0  0  0  0  0  0;
          0  0  0  0  1 -1  0  0  0  0 -1  0  0  0  0  0  0 -1  0  0  0  0  0  0  0  0  0  0  0  0  0  0  0  0;
          0  0  0  0  0  1 -1 -1  0  0  0  0  0  0  0  0  0  0  0  0  0  0  0  0  0  0  0  0  0  0  1  0  0  0;
          0  0  0  0  0  0  0  1  0  0  0  0  0  0  0  0  0  1  1  0  0  0  0  0  0  0  0  0  0  0  0  0  0  0;
          0  0  0  0  0  0  0  0  1 -1 -1  0 -1 -1  0  0  0  0  0  0  0  0  0  0  0  0  0  0  0  0  0  0  0  0;
          0  0  0  0  0  0  0  0  0  1  0 -1  0  0  0  0  0  0  0  0  0  0  0  0  0  0  0  0  0  1  0  0  0  0;
          0  0  0  0  0  0  0  0  0  0  0  0  1  0 -1  0  0  0  0  0  0  0  0  0  1  0  0  0  0  0  0  0  0  0;
          0  0  0  0  0  0  0  0  0  0  0  0  0  0  0  1 -1 -1  0 -1 -1  0  0  0  0  0  0  0  0  0  0  0  0  0;
          0  0  0  0  0  0  0  0  0  0  0  0  0  0  0  0  1  0 -1  0  0  0  0  0  0  0  0  0  1  0  0  0  0  0;
          0  0  0  0  0  0  0  0  0  0  0  0  0  0  0  0  0  0  0  1  0 -1  0  0  1  0  0  0  0  0  0  0  0  0;
          0  0  0  0  0  0  0  0  0  0  0  0  0  0  0  0  0  0  0  0  0  0  1 -1 -1 -1  0  0  0  0  0  0  0  0;
          0  0  0  0  0  0  0  0  0  0  0  0  0  0  0  0  0  0  0  0  0  0  0  0  0  0  1 -1 -1 -1  0  0  0  0;
          0  0  0  0  0  0  1  0  0  0  1  1  0  0  0  0  0  0  0  0  0  0  0  0  0  0  0  0  0  0  0  0  0  0;
         -1  0  0  0 -1  0  0  0  0  0  0 -1  0  0 -1  0  0  0 -1  0  0 -1  0  0  0 -1  0  0  0 -1 -1  0  0  0;
         -1  0 -1  0  0  0 -1  0 -1  0  0  0 -1  0  0  0  0  0  0 -1  0  0 -1 -1  0  0  0 -1  0  0  0 -1  0  0;
          0  0  0 -1 -1  0  0 -1  0 -1  0  0  0  0  0 -1 -1  0  0  0  0  0  0  0 -1  0 -1  0 -1  0  0  0 -1  0;
          0 -1  0  0  0 -1  0  0 -1  0  0  0  0  0  0 -1  0  0  0  0  0  0 -1  0  0  0 -1  0  0  0  0  0  0 -1;
          0  0  0  0  0  0  0  0  0  0  0  0  0  0  0  0  0  0  0  0  0  0  0  0  0  0  0  0  0  0  1  0  0  0;
          0  0  0  0  0  0  0  0  0  0  0  0  0  0  0  0  0  0  0  0  0  0  0  0  0  0  0  0  0  0  0  1  0  0;
          0  0  0  0  0  0  0  0  0  0  0  0  0  0  0  0  0  0  0  0  0  0  0  0  0  0  0  0  0  0  0  0  1  0;
          0  0  0  0  0  0  0  0  0  0  0  0  0  0  0  0  0  0  0  0  0  0  0  0  0  0  0  0  0  0  0  0  0  1];

    n(1) = 0.0055;
    n(2) = 0.0553;
    n(3) = n(1);
    f(1) = 1e-2;
    f(2) = 5e2;
    f(3) = 3;

    rT=3;
```

```
rD=10;
rS=0.1;
areaT = 4*pi*rT^2;
areaD = 4*pi*rD^2;
areaS = pi*rS^2;
D=0.1;
thT=rS/rT;
thD=rS/rD;

f = f*areaS;
n = n*areaS;
f(4) = D/rT^2*(1+cos(thT))/(2*log(2/(1-cos(thT))) - (1+cos(thT)));
f(5) = D/rD^2*(1+cos(thD))/(2*log(2/(1-cos(thD))) - (1+cos(thD)));
n(4) = f(4)*(areaT-areaS);
n(5) = f(5)*(areaD-areaS);

K = [1 2 1 3 3 2 1 3 1 2 2 3 2 2 1 3 2 2 3 2 2 1 2 1 3 1 2 1 3 3 4 5 5 4];

X(1,1:16) = zeros(16,1);
X(1,17:20) = [20000*areaS/areaT; 200*areaS/areaD; 50000*areaS/areaD; 15000*areaS/areaT];
X(1,21:24) = [floor(20000-100*X(17)); floor(200-100*X(18)); floor(50000-100*X(19)); floor(15000-100*X(20))];
for i=17:20
    N=floor(X(i));
    if(rand <= X(i)-N)
        N=N+1;
    end
    X(i)=N;
end

t=0;
T=0:0.0001:Tmax;
Y=zeros(size(T,2),size(X,2));
Y(1,:) = X;
s=2;

tic;
while(t<Tmax)
    C = X;
    C(1:20) = C(1:20)/areaS;
    A = zeros(68,1);

    for i=1:34
        RC=1;
        for j=1:24
            if(V(j,i) == -1)
                RC = RC*C(j);
            end
        end
        A(i) = n(K(i))*RC;
    end
```

```
        for i=1:34
            RC=1;
            for j=1:24
                if(V(j,i) == 1)
                    RC = RC*C(j);
                end
            end
            A(i+34) = f(K(i))*RC;
        end

        a0 = sum(A);
        r = rand(2,1);
        tau = -log(r(1))/a0;
        a0 = a0*r(2);
        asum = cumsum(A);
        m = binsearchf(asum,a0);

        t = t+tau;
        if(m<=34)
            X = X+V(:,m)';
        else
            X = X-V(:,m-34)';
        end
        while(s<=size(T,2) && t>=T(s))
            Y(s,:) = X;
            s=s+1;
        end
    end
    toc;

    c5 = Y(:,3)+Y(:,4)+Y(:,7)+Y(:,16);
    ag = sum(Y(:,1:4),2)+Y(:,3)+sum(Y(:,8:10),2)+Y(:,16);
    se = sum(Y(:,4:7),2)+Y(:,7)+sum(Y(:,11:13),2)+Y(:,16);

    Y = [c5 ag se];
end
```